TMS entrains occipital alpha activity:
Individual alpha frequency predicts the strength of entrained phase-locking

Yong-Jun Lin[1*], Lavanya Shukla[2], Laura Dugué[1-4], Antoni Valero-Cabré[5-7^] & Marisa Carrasco[1,2^]

[1] Department of Psychology, New York University, New York, NY 10003, USA
[2] Center for Neuroscience, New York University, New York, NY 10003, USA
[3] Current : Université de Paris, CNRS, Integrative Neuroscience and Cognition Center, F-75006 Paris, France
[4] Current : Institut Universitaire de France, Paris, France
[5] Cerebral Dynamics, Plasticity and Rehabilitation Group, Frontlab team, Institut du Cerveau et de la Moelle, CNRS UMR 7225, INSERM U 1127 and Sorbonne Université, Paris, France.
[6] Dept. Anatomy and Neurobiology, Laboratory of Cerebral Dynamics, Boston University School of Medicine, Boston, USA
[7] Cognitive Neuroscience and Information Tech. Research Program, Open University of Catalonia, Barcelona, SPAIN

* Corresponding author
^ Joint senior author

E-mails:
yjlin@nyu.edu (YJL)
ls4365@nyu.edu (LS)
laura.dugue@u-paris.fr (LD)
antoni.valerocabre@icm-institute.org (AVC)
marisa.carrasco@nyu.edu (MC)

words: 4000/4000 (w/o abstract/references/title page)
tables: 1
figures: 6
supplementary tables: 1
supplementary figures: 8

Highlights

* online, trial-by-trial entrainment of local neural synchrony in V1/V2 (rhythmic TMS)
* occipital entrainment with concurrent neural stimulation (TMS) and recording (EEG)
* 4-pulse TMS at 10 Hz yields lasting (300 ms) phase-locking at the alpha-band
* individual alpha frequency positively correlated with inter-trial phase coherence

Abstract [248/250]

Background: Parieto-occipital alpha rhythms (8-12 Hz) have been shown to underlie cortical excitability and influence visual performance. However, how the occipital cortex responds to an externally imposed alpha rhythm via transcranial magnetic stimulation (TMS) is an open question.

Hypotheses: 10-Hz rhythmic TMS can entrain intrinsic alpha oscillators in the occipital cortex. Specifically, we predicted: (1) progressive enhancement of entrainment across time windows, (2) output frequency specificity, (3) dependence on the intrinsic oscillation phase, and (4) input frequency specificity to individual alpha frequency (IAF) in the neural signatures.

Methods: We delivered 4-pulse rhythmic TMS at 10 Hz to entrain local neural activity targeting the right V1/V2 regions while participants performed a visual orientation discrimination task. Concurrent electroencephalogram (EEG) recorded TMS-driven changes of local oscillatory activity. There were two control conditions: arrhythmic-active and rhythmic-sham stimulation, both with an equal number of pulses and duration.

Results: The results were consistent with the first three hypotheses. Relative to both controls, rhythmic TMS bursts significantly entrained local neural activity. Near the stimulation site, evoked oscillation amplitude and inter-trial phase coherence (ITPC) was increased for 2 and 3 cycles, respectively, after the last TMS pulse. Critically, regarding hypothesis 4, ITPC following entrainment positively correlated with IAF, rather than with the degree of similarity between IAF and the input frequency (10 Hz).

Conclusions: We entrained alpha-band activity in occipital cortex for ~3 cycles (~300 ms) with our 4-pulse 10 Hz TMS protocol. IAF predicts the strength of entrained occipital alpha phase synchrony indexed by ITPC.

Keywords: Entrainment; alpha-band; transcranial magnetic stimulation (TMS); electroencephalography (EEG); visual discrimination; phosphene; V1/V2

Introduction

Brain oscillations play an important functional role in perception, attention and cognition [1–3]. Specifically, alpha-band (8-12 Hz) neural oscillations reflect ongoing sensory processing. Alpha power inversely correlates with excitability in vision [4–9], audition [10], and somatosensation [11]. In the visual cortex, the parieto-occipital alpha-band phase correlates with baseline cortical excitability (phosphene threshold) [12], gamma-band (40-100 Hz) power [13], and spiking responses [14]. In V1, alpha and gamma rhythms index feedback and feedforward processing, respectively [15,16]. Theories of oscillations postulate that alpha power reflects an active inhibition of task-irrelevant sensory signals [17–19] whereas alpha phase reflects pulsed inhibition [17,20], cyclic perceptual sampling [2] or temporal expectation [21]. Alpha oscillations are often measured but not manipulated. Here we use transcranial magnetic stimulation (TMS) to directly manipulate local alpha rhythms.

The topography of alpha power is altered by spatial attention. Typically, in endogenous (voluntary) spatial attention tasks, alpha power contralateral to the cued visual field shows reduced alpha power while the ipsilateral side shows increased alpha power [22–29]. Moreover, this lateralized alpha power modulation could reach V1 [29,30]. The parieto-occipital alpha-band activity is linked with the allocation of covert spatial attention and receives feedback control from frontoparietal cortices. The disruption of anticipatory pre-stimulus alpha rhythms on the occipital cortex brought about by transcranial magnetic stimulation (TMS) on the right intraparietal sulcus (IPS) or right frontal eye field (FEF) has been associated with deteriorated visual performance [31–33]. With Granger causality analyses applied to magnetoencephalogram data, alpha power modulation in the right FEF has been reported to predict alpha activity in V1, indicating feedback control [34]. Thus, V1/V2 may receive feedback control from FEF and IPS, two crucial nodes of the dorsal attention network.

Entrainment –the progressive phase alignment of intrinsic oscillators by external sources of rhythmic stimulation (reviews [35–37])– has been proposed to underlie top-down modulations of

93 attention [38–44]. Although visual signals in visuo-occipital areas are modulated by attention [45–
94 48], a fundamental question is whether and how the occipital cortex would respond to entrainment
95 while participants perform a visual task, even without attention being explicitly manipulated. To
96 address this question, we utilized a short-burst rhythmic TMS protocol along with concurrent EEG
97 recordings [44,49], targeting V1/V2 with visual field mapping by fMRI and/or phosphene induction.
98 For the frequency of alpha-band stimulation, previous short-burst TMS studies used either
99 10 Hz [50,51] or individual alpha frequency (IAF) as the entrainment frequency [49,52]. IAF is a
100 stable neurophysiological trait marker at rest [53], which increases with task demand [54,55] and
101 reflects the task-required temporal integration window [56]. However, the assumption that matching
102 the entraining frequency with IAF is important has not been directly tested in concurrent TMS-EEG
103 studies [37]. Our strategy was to use 10 Hz as the entraining frequency and examine whether the
104 degree of similarity between IAF and 10 Hz predicted the magnitude of phase-locked activities
105 following entrainment.
106 Here we asked how the occipital cortex responds to entrainment while controlling spatial
107 attention allocation to be distributed across the left and right visual fields, where the stimuli
108 appeared. We aimed to entrain alpha-band synchrony in early visual areas with rhythmic 10 Hz
109 TMS and examine the neural signatures of entrainment with EEG. We hypothesized that the
110 occipital alpha-band activity can be entrained by targeting V1/V2 because intrinsic alpha oscillators
111 exist in V1 [14,57] and V2 [58]. Given that V1/V2 play a pivotal role in early visual information
112 processing, it is important to find out whether entrainment with rhythmic TMS can be established in
113 these areas and how long such entrainment would last. We adopted arrhythmic-active TMS and
114 rhythmic-sham stimulation control conditions, similar to previous TMS-EEG entrainment studies
115 [44,49]. We systematically analyzed the temporal dynamics in multiple time windows during and
116 after stimulation bursts. Although modulations of neural activity do not necessarily lead to changes
117 in behavior, our secondary goal was to examine whether entrained alpha-band oscillations

118 targeting early visual cortex (V1/V2) could affect perceptual discriminability and/or criteria in a
119 visual discrimination task.
120 Based on our hypothesis that occipital alpha-band activity can be entrained by targeting
121 V1/V2 with 10 Hz TMS bursts, we tested four specific predictions characterizing TMS-driven
122 entrainment (the first three have been previously tested in frontal and parietal locations [44,49]): (1)
123 *Progressive enhancement of entrainment*: the strength of phase-locked activity, as measured by
124 evoked (phase-locked) oscillation amplitude (as opposed to induced, non-phase-aligned,
125 oscillation amplitude, [59]) and ITPC (consistency of phase alignment) [44,49], should be
126 enhanced only after the second TMS pulse of the 4-pulse burst), because the alpha periodicity of
127 the entraining rhythm is not defined until then. Otherwise, the results could simply reflect phase-
128 resetting due to the first TMS pulse. (2) *Output frequency specificity*: entrained phase-locked
129 activity should peak around the 10-Hz TMS frequency. (3) *Dependence on the intrinsic oscillation*
130 *phase:* entrained activity should depend on the pre-TMS alpha phase [49]. Were the enhanced
131 phase-locked activity due to reverberation of the imposed rhythm, rather than entrainment of
132 intrinsic oscillators, the entrained activity should be similar regardless of pre-TMS alpha phase. (4)
133 *Input frequency specificity*: The strength of the entrained activity should correlate with the degree
134 of similarity between IAF and 10 Hz, given that IAF may be the intrinsic oscillation frequency of
135 occipital alpha oscillators [49].
136
137 **Materials and Methods**
138
139 **Participants**
140 All 11 participants (5 female; 9 naïve to the purpose of the study; 20-47 years; M=29.9;
141 SD=6.8) provided written informed consent. One participant's data were excluded due to excessive
142 involuntary blinking. NYU institutional review board approved the protocol (IRB #i14-00788), which
143 followed the Declaration of Helsinki and safety guidelines for TMS experiments [60].

144

145 **Apparatus**

146 The stimuli were presented on a ViewSonic P220f monitor. The screen resolution was
147 800(H)x600(V) at 120Hz. The viewing distance was 57 cm, set by a chin-rest. The stimuli
148 presentation code was written in MATLAB with Psychtoolbox 3 [61,62]. To linearize stimuli
149 contrast, the monitor's gamma function was measured with a ColorCAL MKII Colorimeter
150 (Cambridge Research Systems). The TMS pulses were delivered with a 70-mm figure-of-eight coil
151 controlled by a Magstim Super Rapid^2 Plus^1 system. The EEG system consisted of a Brain
152 Products actiCHamp amplifier and TMS-compatible Easycap actiCAP slim caps. See
153 Supplementary Methods for TMS coil positioning and neuronavigation, as well as for the EEG cap
154 layout, impedance, and event timing precision (**Figure S1A**).

155

156 **Visual discrimination task**

157 The participants performed an orientation discrimination task. Each trial began with a
158 fixation period, followed by a 30-ms neutral pre-cue indicating that the target could be either in the
159 lower left or lower right visual field with equal probability (**Figure 1a**). After a brief inter-stimulus
160 interval (ISI), two Gabor patches and a response cue, indicating which patch was the target,
161 appeared simultaneously. The Gabor patches (achromatic; 4 cpd; σ 0.42°) lasted 50 ms.
162 Participants were asked to indicate whether the target patch was slightly clockwise or
163 counterclockwise relative to vertical via a key press (right index finger for the '/' key; left index
164 finger for the 'z' key).

165 A central fixation cross was constantly present. Participants were asked to maintain fixation
166 at all times and to blink after each trial. An eye tracker (EyeLink1000) ensured that fixation was
167 within a 1.5° radius invisible circle. Trials for which fixation was broken (including blinking), from
168 cue onset to stimuli offset, were discarded and repeated at the end of the block. The contrast level
169 of the two Gabor patches were independently titrated before the experiment. A method of constant

170 stimuli (4-80% Gabor contrasts in 7 log steps) was used to obtain the contrast at which sensitivity
171 (d') [63,64] reached half-of-max sensitivity of the Naka-Rushton function was defined as c_{50}
172 contrast. The group average (standard deviation) of c_{50} contrast was 16% (4%) for both visual
173 fields.

174 During the ISI, 4 rhythmic or arrhythmic, active or sham pulses were delivered. Participants
175 could not tell the sound difference wearing ear plugs. The experimental design was within-subject.
176 The rhythmic and arrhythmic stimulations were blocked. The stimulation type (active or sham) and
177 the target side were randomized within blocks. The experiment consisted of 8 blocks, each
178 contained 64 trials, for a total of 512 trials; 128 trial repetitions per each of the 4 experimental
179 conditions (2 rhythmicity types × 2 stimulation types).

180 For the secondary goal, we found no significant effects regarding whether entrainment
181 modulates visual discrimination [63,64], either for visual sensitivity (d'; **Figure S2**) or response
182 criterion (c; **Figure S3**). The error bars represent ±1 S.E.M. corrected for within-subject design [65].
183

184 **Transcranial magnetic stimulation**

185 The TMS site for each participant was defined by retinotopy or phosphenes (see Supplementary
186 Methods). **Figure 1c** illustrates the vectors connecting the cortical and scalp sites for each
187 participant. All but one participant's stimulation vector clustered around electrodes Oz, O2 and
188 PO4. The TMS intensity was fixed at 70% for all participants (except for one at 65% and another at
189 67%) of the maximal machine output, to ensure no phosphene induction during the task. The sham
190 control consisted of 4 pulses of pre-recorded TMS sounds played through a speaker attached to
191 the coil. Participants were asked to report if they saw any phosphenes at any point during the task;
192 they reported none.

193 In the rhythmic condition, the pulses were 100 ms apart, aiming to induce alpha-band
194 entrainment. In the arrhythmic condition, the timing of the first and last pulses of the burst were the
195 same as in the rhythmic condition, whereas the timing of the second and the third pulses were

196 randomly jittered on each trial according to a bimodal distribution synthesized from normal
197 distributions N (±30ms, 10ms) (**Figure S1B**). Before and after the experiment, we verified that the
198 registered TMS timings on the EEG achieved the expected precision (**Figures S1C-D**).
199
200 **EEG recordings and analyses**
201 Before the experiment, we recorded 2-min eyes-closed resting-state activity to define the
202 individual alpha frequency (IAF) as the frequency corresponding to the maximum peak between 7
203 and 13 Hz on Welch's periodogram [66] (MATLAB command: pwelch). The EEG recordings were
204 digitized at 2500 Hz and down-sampled offline to 100 Hz for further analyses. All analyses were
205 carried out with MATLAB R2017a and software packages FieldTrip [67] and Brainstorm [68]. The
206 TMS artifacts were removed by interpolation (see Supplementary Methods). The continuous data
207 were then segmented into epochs containing data from 300 ms before to 900 ms after the neutral
208 pre-cue.
209 To assess if the neural activity was phase-locked to the entraining periodic stimulation, we
210 calculated two indices for each of the 4 conditions: (1) evoked oscillatory amplitude (square-root of
211 power), by averaging waveforms across trials first and then applying Morlet wavelets [59]; (2) inter-
212 trial phase coherence (ITPC, or phase-locking value) [69] by applying Morlet wavelets to each trial
213 and calculating their consistency with $\sum_{i=1}^{N} e^{i\theta}/N$, where i denotes the trial number, N the total
214 number of trials, and θ the phase. ITPC is a ratio between 0 and 1, in which 1 indicates perfect
215 phase alignment. For both indices, each Morlet wavelet had 5 cycles, and the frequency range was
216 3-50 Hz.
217 We analyzed the evoked oscillation amplitude and ITPC in 7 planned time windows: W0 (5-
218 105ms, before the first pulse), W1 (105-205ms, between the first and second pulses), W2 (205-
219 305ms, between the second and third pulses), W3 (305-405ms, between the third and last pulses),
220 W4 (405-505ms, first cycle after the last pulse), W5 (505-605ms, second cycle after the last pulse),
221 and W6 (605-705ms, third cycle after the last pulse). These planned time windows are consistent

222 with reported time intervals of entrainment effects by TMS [44,49,51]. The planned contrasts were
223 corrected for multiple comparisons within, but not across, time windows. Within each time window,
224 topographic analyses were corrected for multiple comparison across channels with cluster-based
225 permutation tests [70]. According to the trial structure of the visual discrimination task, stimuli were
226 presented in the middle of W2 (530-580 ms). Online eye tracking ensured that the trials containing
227 eye blinking were discarded so that the analyzed EEG time windows were free of such artifacts.

228 Several statistical tests were performed. (1) As entrainment should lead to localized
229 elevation of evoked oscillation amplitude and ITPC near the stimulation site, t-tests were performed
230 by averaging the neural signatures in channels O2 and PO4 in the 10-Hz band at all time windows.
231 (2) To explore the temporal and spectral specificity of entrainment, t-tests of the two neural
232 signatures were performed across all time-frequency bins averaged across channels O2 and PO4.
233 (3) To explore the topography of neural activity before, during and after entrainment, t-tests were
234 performed across all channels in the 10 Hz band at all time windows. (4) To examine whether ITPC
235 enhancement following rhythmic TMS depended on pre-TMS (200 ms before the first pulse) alpha
236 phase, ITPC across participants and time points in W2-W6 were assorted into 6 equidistant 10 Hz
237 phase bins for one-way repeated measures ANOVA and a regression analysis with a sine wave (y
238 $= a*\sin(f*x*\pi/3+\phi)+c$, where x is the bin number; a, f, ϕ, and c were free parameters) [49]. (5) To
239 examine the relation between IAF and ITPC, a linear regression was performed.

240 For the rhythmic-active condition, the arrhythmic-active condition is a more stringent control
241 than the rhythmic-sham condition across all figures (**Figures 2, 4-6, S4-S7**) (see also [49]). Across
242 all time windows (**Figures 4-6, S4-S7**), the contrasts between the rhythmic-active and arrhythmic-
243 active conditions were significant whenever those between the rhythmic-active and rhythmic-sham
244 condition were significant, except for evoked oscillation amplitude and ITPC in W0 and evoked
245 oscillation amplitude in W1 (**Figures S4, S5A**). Therefore, we report the statistical contrast
246 between the rhythmic and arrhythmic-active stimulation conditions.
247

248 **Results**

249 We present analyses relevant for each of the 4 hypotheses, followed by exploratory
250 analyses regarding the temporal dynamics of the topography of the entrainment effect. Altogether
251 both sets of results indicate successful entrainment.

252 *(1) Progressive enhancement of entrainment.* To evaluate the temporal evolution of
253 entrainment, we obtained t-test results of the planned contrasts between rhythmic and arrhythmic-
254 active stimulation conditions in the 7 pre-defined time windows (**Materials and Methods**) for
255 evoked oscillation amplitude and ITPC (**Table 1**). Consistent with our prediction regarding
256 entrained neural activity, the planned contrasts were not statistically significant 100-ms before and
257 after the first TMS pulse (W0 and W1, p>.05), but became significantly different for the later time
258 windows (W2, W3, and W4, p<.05). Interestingly, the occipital alpha-band stimulation enhanced
259 phase-locked activity during the second and the third cycles after the last pulse (significant
260 contrasts in W5 and W6, p<.05). Our entrainment effect in terms of both evoked oscillation
261 amplitude and ITPC was long lasting (200 and 300 ms, respectively, after the last pulse of the TMS
262 burst).

263 *(2) Output frequency specificity of entrainment*. To assess the output frequency-specificity,
264 we conducted time-frequency analysis of phase-locked activities with frequencies ranging 3-50 Hz
265 and time ranging 0-750 ms (**Figure 2**). Rhythmic-active stimulation elicited activity at ~10 Hz and
266 its first harmonic (~20 Hz). Additionally, there were broad band responses for each of the 4 TMS
267 pulses. Overall, the patterns for evoked oscillation amplitude and ITPC (**Figure 2A,B**) were similar.

268 *(3) Dependence on the intrinsic oscillation phase*. To ensure that the enhanced phase-
269 locked activity reflected entrainment rather than reverberation of an externally imposed rhythm, we
270 performed regression analyses on ITPC across the time windows that were significant (W2-W6) in
271 **Table 1**. The pre-TMS phases (200 ms before the first 10-Hz pulse) were assorted into 6
272 equidistant phase bins [49]. One-way repeated measures ANOVA revealed that the ITPC values
273 across phase bins were significantly different [$F(9,45)=6.67$, $P<1e-5$]. In this period, ITPC

depended on the phase bin with a sinusoidal trend (**Figure 3A)**, as previously reported [49], suggesting that the phase of ongoing alpha oscillations matters. This result refutes the reverberation account, according to which ITPC would have been a flat line.

(4) Input frequency dependence of entrainment. Inconsistent with the hypothesis that the intrinsic oscillators operate at the IAF in the occipital cortex, the degree of similarity between IAF and 10 Hz did not correlate with entrained ITPC (**Figure 3B**). Instead, IAF directly correlated with entrained ITPC (**Figure 3C**). The correlations of IAF with ITPC or with evoked oscillation amplitude were not significant (**Figure S8**).

Topography. We explored the topography of the entrainment effects by performing topographic analysis of phase-locked alpha-band activities in each time window and assessing the temporal dynamics of evoked oscillation amplitude and ITPC. Cluster-based permutation tests [70] were used for correction of multiple comparisons. Descriptively, with the same alpha threshold for cluster-based permutation test, 10-Hz activity was initially widespread, likely due to EEG volume conduction, and progressively became more local over time. The statistically significant cluster included the frontal and occipital regions for both evoked oscillation amplitude and ITPC in W2-W4 (**Figures 4, S6-S7**). Note that the occipital clusters in W2-W6 (**Figures 4-6, S5-S6**) were more lateralized towards the stimulated (right) side. See Supplementary Results for converging evidence of lasting entrainment effects.

Discussion

This study is the first to show TMS entrainment of alpha activity in occipital cortex. We evaluated whether occipital alpha-band activity can be entrained by TMS targeting V1/V2 while participants performed a visual discrimination task. We tested the following hypotheses, based on established entrainment characteristics: (1) *progressive enhancement of entrainment*, (2) *output frequency specificity*, (3) *dependence on the intrinsic oscillation phase*, and (4) *input frequency*

300 *specificity*. Our results are consistent with the first three hypotheses, revealing that occipital alpha
301 activity can be entrained. However, the results were not consistent with the 4th hypothesis. Instead,
302 IAF correlated with ITPC.
303
304 **Lasting alpha-band phase-locking in the occipital cortex**
305 With a 4-pulse 10-Hz TMS protocol, we successfully entrained the right occipital cortex for 3
306 cycles (300 ms) after the last TMS pulse. This novel result reveals that short-burst rhythmic TMS
307 can effectively entrain frequency-specific neural synchrony in the stimulated region. In previous
308 concurrent TMS-EEG studies [44,49,51,71,72], short-burst rhythmic TMS elicited evoked oscillation
309 amplitude for 1-2 cycles using an entraining frequency matching the natural oscillatory frequency of
310 the target brain region. Note that our results fulfilled entrainment requirements and ruled out a
311 reverberation account (as in [49]). Moreover, the evoked oscillation amplitude and ITPC at the
312 alpha-band were not significantly different between the rhythmic and arrhythmic-active stimulation
313 conditions in time windows W0 and W1. Therefore, it is unlikely that the lasting effects we found
314 were due to temporal leakage of wavelets. We may have obtained longer lasting TMS-entrained
315 duration than the study entraining right IPS [49] because our participants were engaged in a visual
316 task, instead of in resting state. The only study evaluating TMS entrainment in occipital cortex
317 reported not to find it [51], even though their participants were also engaged in a visual
318 discrimination task; their 3 10-Hz TMS pulses may have been insufficient for entraining the occipital
319 cortex.
320 Our results reveal that changes of two phase-locked activity measures –evoked oscillation
321 amplitude and ITPC– show different temporal dynamics beyond the stimulation burst. ITPC lasted
322 one more cycle than evoked oscillation amplitude (**Table 1**; **Figures 2,5,6**). As ITPC is a phase-
323 locking activity measure that does not take amplitude into account, this finding suggests that phase
324 could be more sensitive and informative than amplitude to index the occurrence and duration of
325 entrainment effects in the occipital cortex.

The finding that the occipital cortex can be entrained by TMS is consistent with the notion of inter-areal entrainment as a form of neural communication whose function could be to achieve local phase alignment [36,38]. Given that visual stimuli were presented at the same timing across all conditions, the continued phase-locking in the second and third cycles after the last pulse (W5 and W6) cannot be attributed to evoked alpha activity by target onset.

IAF directly predicts occipital entrainment

Some studies have assumed that using IAF, the intrinsic oscillation frequency of the parieto-occipital cortex at rest, as the entraining frequency would be optimal for entrainment, but this assumption has rarely been tested [37]. Overall, our findings are inconsistent with such an assumption: The dependency of ITPC on pre-TMS phase shows that entrainment effects depend on the ongoing oscillatory state while participants are engaged in a visual task, refuting a passive reverberation account (**Figure 3A**). Therefore, intrinsic alpha oscillators exist in the occipital cortex. However, the parieto-occipital alpha rhythm does not necessarily possess a unitary IAF and their cortical sources can be decomposed into occipito-parietal and occipito-temporal [73] or parietal and occipital [54] components. Were IAF the intrinsic occipital oscillator frequency, smaller differences between IAF and the fixed 10-Hz entrained frequency should have led to greater ITPC. However, their null correlation did not support this hypothesis (**Figure 3B**). Instead, we found a direct positive correlation between IAF and ITPC (**Figure 3C**), which suggests that individuals with higher IAF may be more susceptible to occipital alpha-band entrainment.

Can alpha-band occipital TMS entrainment modulate visual sensitivity (d')?

Our results show that visual sensitivity in a discrimination task was unaffected by the elevated alpha-band evoked oscillation amplitude and ITPC (**Figures S2** and **S3**). Given that we only tested one specific target presentation timing, and at one TMS intensity per participant, our result does not necessarily rule out the possibility that changes in phase-locked activity level could

352 modulate d'. For instance, a study showed that hit rate, but not false alarm rate, in the visual field
353 ipsilateral to TMS was significantly higher immediately after a 5-pulse alpha-band TMS over the
354 occipital cortex than that in the sham condition [50]. Likewise, after alpha-band visual flicker,
355 discrimination accuracy oscillates ~10 Hz [74,75]. Thus, the testing of multiple time lags at multiple
356 intensities, as well as entraining other locations (e.g., electrode CP4), stimulating at different
357 frequencies (e.g., theta), or manipulating spatial attention [47,48,76] could inform whether accuracy
358 oscillates after occipital TMS entrainment and whether more elevated evoked oscillation amplitude
359 and ITPC are required for a significant behavioral outcome.
360 In contrast to phase-locked analyses, some visual detection studies with trial-by-trial
361 spontaneous oscillation analysis have revealed that pre-stimulus alpha power [77,78] and phase
362 [79] correlate with response criterion (c) instead of visual sensitivity (d'). Further, for visual
363 discrimination tasks, pre-stimulus alpha power correlates with confidence instead of accuracy [80].
364 However, note that without entrainment, trial-by-trial spontaneous pre-stimulus alpha activity is
365 random and hence non-phase-locked across trials. Therefore, the current findings do not
366 necessarily negate the possibility that entrainment may alter d' following alpha-band entrainment.
367
368 **Protocol considerations for future studies**
369 An advantage of our protocol is that it has an arrhythmic-active stimulation control
370 condition, similar to those when investigating IPS [49] and FEF [44] areas. Across time windows,
371 using the arrhythmic-active and rhythmic-sham control conditions led to similar statistical
372 outcomes; overall, the arrhythmic-active condition was a more stringent control condition resulting
373 in less widespread significant statistical differences at the scalp level (**Figures 2, 4-6, S4-S7**).
374 Across the topographic analyses (except in W5, **Figure 5B)**, the rhythmic and arrhythmic-sham
375 stimulation conditions did not significantly differ, implying that the sound pulses alone cannot
376 explain the entrainment of phase-locked activity. Therefore, follow-up studies may consider
377 removing the sham conditions to increase the statistical power of different types of TMS trials.

Our 4-pulse alpha-band TMS protocol provides an interesting alternative for occipital entrainment to that of transcranial alternating current stimulation (tACS) protocols. Alpha-band tACS protocols typically involves 10-20 minutes of stimulation followed by 1-3 minutes of testing period, during which enhanced alpha-power or ITPC has been recorded with concurrent EEG and taken as evidence of entrainment [81,82] (but see alternative interpretations: [83,84]). In any case, TMS protocols [49,51], including ours, provide more focal stimulation effects than tACS and can be effectively delivered in shorter 'bursts' of pulses, hence pinpoint more accurately the temporal dynamics of entrainment effects, enable trial-by-trial stimulation designs and concurrent EEG recordings.

Conclusion

We have established a rhythmic 4-pulse alpha-band occipital TMS protocol for effective trial-by-trial, online brain stimulation to enable alpha entrainment in retinotopically organized V1/V2 areas. With a 300-ms entraining period, phase-locked activities persisted for ~300 ms (three 10-Hz cycles) after the last pulse. To our knowledge, this is the most effective short-burst TMS entrainment finding up to date. Moreover, we found that IAF predicts the strength of entrained phase-locking across trials (ITPC). Therefore, IAF is a key factor worth investigating in future alpha entrainment studies.

CRediT authorship contribution statement

Yong-Jun Lin: Conceptualization, Methodology, Software, Formal analysis, Investigation, Resources, Data Curation, Writing - Original Draft (with guidance and supervision from M. C.), Visualization

Lavanya Shukla: Software, Investigation, Data Curation

Laura Dugué: Conceptualization, Methodology, Writing - Review & Editing

Antoni Valero-Cabré: Conceptualization, Methodology, Writing - Review & Editing, Supervision

Marisa Carrasco: Conceptualization, Methodology, Writing - Review & Editing, Supervision, Project administration, Funding acquisition

Acknowledgements

This research was supported by National Institute of Health (NIH R21-EY026185-01A1) to MC, IHU-A-ICM-Translationnel, ANR projet Générique OSCILOSCOPUS and Flag-era-JTC-2017 CAUSALTOMICS to AVC. We thank Antonio Fernández and Zhilin Zhang for assistance in data collection; Noah Benson and Marc Himmelberg for guidance on fMRI retinotopy data analysis; Antonio Fernández and Chloé Stengel for valuable discussions regarding this project; Rachel Denison and Florencia Assaneo for useful comments on the manuscript.

Commercial relationships: none.

References

[1] Buzsáki G. Rhythms of the brain. New York: Oxford University Press; 2006.

[2] VanRullen R. Perceptual cycles. Trends Cogn Sci 2016;20:723–35. https://doi.org/10.1016/j.tics.2016.07.006.

[3] Dugué L, VanRullen R. Transcranial magnetic stimulation reveals intrinsic perceptual and attentional rhythms. Front Neurosci 2017;11:154. https://doi.org/10.3389/fnins.2017.00154.

[4] Ergenoglu T, Demiralp T, Bayraktaroglu Z, Ergen M, Beydagi H, Uresin Y. Alpha rhythm of the EEG modulates visual detection performance in humans. Cogn Brain Res 2004;20:376–83. https://doi.org/10.1016/j.cogbrainres.2004.03.009.

[5] Hanslmayr S, Klimesch W, Sauseng P, Gruber W, Doppelmayr M, Freunberger R, et al. Visual discrimination performance is related to decreased alpha amplitude but increased phase locking. Neurosci Lett 2005;375:64–8. https://doi.org/10.1016/j.neulet.2004.10.092.

[6] Hanslmayr S, Aslan A, Staudigl T, Klimesch W, Herrmann CS, Bäuml K-H. Prestimulus oscillations predict visual perception performance between and within subjects. NeuroImage 2007;37:1465–73. https://doi.org/10.1016/j.neuroimage.2007.07.011.

[7] Rahn E, Başar E. Enhancement of visual evoked potentials by stimulation during low prestimulus EEG stages. Int J Neurosci 1993;72:123–36. https://doi.org/10.3109/00207459308991629.

[8] Romei V, Brodbeck V, Michel C, Amedi A, Pascual-Leone A, Thut G. Spontaneous fluctuations in posterior α-band EEG activity reflect variability in excitability of human visual areas. Cereb Cortex 2008;18:2010–8. https://doi.org/10.1093/cercor/bhm229.

[9] Romei V, Rihs T, Brodbeck V, Thut G. Resting electroencephalogram alpha-power over posterior sites indexes baseline visual cortex excitability. Neuroreport 2008;19:203–8. https://doi.org/10.1097/WNR.0b013e3282f454c4.

[10] Rahn E, Başar E. Prestimulus EEG-activity strongly influences the auditory evoked vertex response A new method for selective averaging. Int J Neurosci 1993;69:207–20. https://doi.org/10.3109/00207459309003331.

[11] Ploner M, Gross J, Timmermann L, Pollok B, Schnitzler A. Oscillatory activity reflects the excitability of the human somatosensory system. NeuroImage 2006;32:1231–6. https://doi.org/10.1016/j.neuroimage.2006.06.004.

[12] Dugué L, Marque P, VanRullen R. The phase of ongoing oscillations mediates the causal relation between brain excitation and visual perception. J Neurosci 2011;31:11889–93. https://doi.org/10.1523/JNEUROSCI.1161-11.2011.

[13] Osipova D, Hermes D, Jensen O. Gamma power is phase-locked to posterior alpha activity. PLoS ONE 2008;3:e3990. https://doi.org/10.1371/journal.pone.0003990.

[14] Dougherty K, Cox MA, Ninomiya T, Leopold DA, Maier A. Ongoing alpha activity in V1 regulates visually driven spiking responses. Cereb Cortex 2017;27:1113–24. https://doi.org/10.1093/cercor/bhv304.

[15] Michalareas G, Vezoli J, van Pelt S, Schoffelen J-M, Kennedy H, Fries P. Alpha-beta and gamma rhythms subserve feedback and feedforward influences among human visual cortical areas. Neuron 2016;89:384–97. https://doi.org/10.1016/j.neuron.2015.12.018.

[16] van Kerkoerle T, Self MW, Dagnino B, Gariel-Mathis M-A, Poort J, van der Togt C, et al. Alpha and gamma oscillations characterize feedback and feedforward processing in monkey visual cortex. Proc Natl Acad Sci U S A 2014;111:14332–41. https://doi.org/10.1073/pnas.1402773111.

[17] Jensen O, Mazaheri A. Shaping functional architecture by oscillatory alpha activity Gating by inhibition. Front Hum Neurosci 2010;4:186. https://doi.org/10.3389/fnhum.2010.00186.

[18] Klimesch W, Sauseng P, Hanslmayr S. EEG alpha oscillations The inhibition-timing hypothesis. Brain Res Rev 2007;53:63–88. https://doi.org/10.1016/j.brainresrev.2006.06.003.

[19] Palva S, Palva JM. New vistas for α-frequency band oscillations. Trends Neurosci 2007;30:150–8. https://doi.org/10.1016/j.tins.2007.02.001.

[20] Kizuk SAD, Mathewson KE. Power and phase of alpha oscillations reveal an interaction between spatial and temporal visual attention. J Cogn Neurosci 2017;29:480–94. https://doi.org/10.1162/jocn_a_01058.

[21] Rohenkohl G, Nobre AC. Alpha oscillations related to anticipatory attention follow temporal expectations. J Neurosci 2011;31:14076–84. https://doi.org/10.1523/JNEUROSCI.3387-11.2011.

[22] Gould IC, Rushworth MF, Nobre AC. Indexing the graded allocation of visuospatial attention using anticipatory alpha oscillations. J Neurophysiol 2011;105:1318–26. https://doi.org/10.1152/jn.00653.2010.

[23] Ikkai A, Dandekar S, Curtis CE. Lateralization in alpha-band oscillations predicts the locus and spatial distribution of attention. PLoS ONE 2016;11:e0154796. https://doi.org/10.1371/journal.pone.0154796.

[24] Kelly SP, Lalor EC, Reilly RB, Foxe JJ. Increases in alpha oscillatory power reflect an active retinotopic mechanism for distracter suppression during sustained visuospatial attention. J Neurophysiol 2006;95:3844–51. https://doi.org/10.1152/jn.01234.2005.

[25] Rihs TA, Michel CM, Thut G. Mechanisms of selective inhibition in visual spatial attention are indexed by α-band EEG synchronization. Eur J Neurosci 2007;25:603–10. https://doi.org/10.1111/j.1460-9568.2007.05278.x.

[26] Sauseng P, Klimesch W, Stadler W, Schabus M, Doppelmayr M, Hanslmayr S, et al. A shift of visual spatial attention is selectively associated with human EEG alpha activity. Eur J Neurosci 2005;22:2917–26. https://doi.org/10.1111/j.1460-9568.2005.04482.x.

[27] Thut G, Nietzel A, Brandt SA, Pascual-Leone A. α-band electroencephalographic activity over occipital cortex indexes visuospatial attention bias and predicts visual target detection. J Neurosci 2006;26:9494–502. https://doi.org/10.1523/JNEUROSCI.0875-06.2006.

[28] Worden MS, Foxe JJ, Wang N, Simpson GV. Anticipatory biasing of visuospatial attention indexed by retinotopically specific α-band electroencephalography increases over occipital cortex. J Neurosci 2000;20:RC63. https://doi.org/10.1523/JNEUROSCI.20-06-j0002.2000.

[29] Yamagishi N, Goda N, Callan DE, Anderson SJ, Kawato M. Attentional shifts towards an expected visual target alter the level of alpha-band oscillatory activity in the human calcarine cortex. Cogn Brain Res 2005;25:799–809. https://doi.org/10.1016/j.cogbrainres.2005.09.006.

[30] Yamagishi N, Callan DE, Goda N, Anderson SJ, Yoshida Y, Kawato M. Attentional modulation of oscillatory activity in human visual cortex. NeuroImage 2003;20:98–113. https://doi.org/10.1016/s1053-8119(03)00341-0.

[31] Capotosto P, Babiloni C, Romani GL, Corbetta M. Frontoparietal cortex controls spatial attention through modulation of anticipatory alpha rhythms. J Neurosci 2009;29:5863–72. https://doi.org/10.1523/JNEUROSCI.0539-09.2009.

[32] Capotosto P, Babiloni C, Romani GL, Corbetta M. Differential contribution of right and left parietal cortex to the control of spatial attention A simultaneous EEG-rTMS study. Cereb Cortex 2012;22:446–54. https://doi.org/10.1093/cercor/bhr127.

[33] Marshall TR, O'Shea J, Jensen O, Bergmann TO. Frontal eye fields control attentional modulation of alpha and gamma oscillations in contralateral occipitoparietal cortex. J Neurosci 2015;35:1638–47. https://doi.org/10.1523/JNEUROSCI.3116-14.2015.

[34] Popov T, Kastner S, Jensen O. FEF-controlled alpha delay activity precedes stimulus-induced gamma-band activity in visual cortex. J Neurosci 2017;37:4117–27. https://doi.org/10.1523/JNEUROSCI.3015-16.2017.

[35] Thut G, Bergmann TO, Fröhlich F, Soekadar SR, Brittain J-S, Valero-Cabré A, et al. Guiding transcranial brain stimulation by EEG/MEG to interact with ongoing brain activity and associated functions A position paper. Clin Neurophysiol 2017;128:843–57. https://doi.org/10.1016/j.clinph.2017.01.003.

[36] Lakatos P, Gross J, Thut G. A new unifying account of the roles of neuronal entrainment. Curr Biol 2019;29:R890–905. https://doi.org/10.1016/j.cub.2019.07.075.

[37] Fröhlich F. Experiments and models of cortical oscillations as a target for noninvasive brain stimulation. Prog Brain Res 2015;222:41–73. https://doi.org/10.1016/bs.pbr.2015.07.025.

[38] Calderone DJ, Lakatos P, Butler PD, Castellanos FX. Entrainment of neural oscillations as a modifiable substrate of attention. Trends Cogn Sci 2014;18:300–9. https://doi.org/10.1016/j.tics.2014.02.005.

[39] Lakatos P, Karmos G, Mehta AD, Ulbert I, Schroeder CE. Entrainment of neuronal oscillations as a mechanism of attentional selection. Science 2008;320:110–3. https://doi.org/10.1126/science.1154735.

[40] Fries P. Rhythms for cognition Communication through coherence. Neuron 2015;88:220–35. https://doi.org/10.1016/j.neuron.2015.09.034.

[41] Chanes L, Chica AB, Quentin R, Valero-Cabré A. Manipulation of pre-target activity on the right frontal eye field enhances conscious visual perception in humans. PLoS ONE 2012;7:e36232. https://doi.org/10.1371/journal.pone.0036232.

[42] Chanes L, Quentin R, Tallon-Baudry C, Valero-Cabré A. Causal frequency-specific contributions of frontal spatiotemporal patterns induced by non-invasive neurostimulation to human visual performance. J Neurosci 2013;33:5000–5. https://doi.org/10.1523/JNEUROSCI.4401-12.2013.

[43] Quentin R, Frankston SE, Vernet M, Toba MN, Bartolomeo P, Chanes L, et al. Visual contrast sensitivity improvement by right frontal high-beta activity is mediated by contrast gain mechanisms and influenced by fronto-parietal white matter microstructure. Cereb Cortex 2016;26:2381–90. https://doi.org/10.1093/cercor/bhv060.

[44] Vernet M, Stengel C, Quentin R, Amengual JL, Valero-Cabré A. Entrainment of local synchrony reveals a causal role for high-beta right frontal oscillations in human visual consciousness. Sci Rep 2019;9:14510. https://doi.org/10.1038/s41598-019-49673-1.

[45] Beck DM, Kastner S. Neural systems for spatial attention in the human brain: Evidence from neuroimaging in the framework of biased competition. Oxf. Handb. Atten. 1st ed., New York: Oxford University Press; 2014.

[46] Chica AB, Bartolomeo P, Lupiáñez J. Two cognitive and neural systems for endogenous and exogenous spatial attention. Behav Brain Res 2013;237:107–23. https://doi.org/10.1016/j.bbr.2012.09.027.

[47] Dugué L, Merriam EP, Heeger DJ, Carrasco M. Differential impact of endogenous and exogenous attention on activity in human visual cortex. Sci Rep 2020;10:21274. https://doi.org/10.1038/s41598-020-78172-x.

[48] Fernández A, Carrasco M. Extinguishing exogenous attention via transcranial magnetic stimulation. Curr Biol 2020;30:1–7. https://doi.org/10.1016/j.cub.2020.07.068.

[49] Thut G, Veniero D, Romei V, Miniussi C, Schyns P, Gross J. Rhythmic TMS causes local entrainment of natural oscillatory signatures. Curr Biol 2011;21:1176–85. https://doi.org/10.1016/j.cub.2011.05.049.

[50] Romei V, Gross J, Thut G. On the role of prestimulus alpha rhythms over occipito-parietal areas in visual input regulation Correlation or causation? J Neurosci 2010;30:8692–7. https://doi.org/10.1523/JNEUROSCI.0160-10.2010.

[51] Jaegle A, Ro T. Direct control of visual perception with phase-specific modulation of posterior parietal cortex. J Cogn Neurosci 2014;26:422–32. https://doi.org/10.1162/jocn_a_00494.

[52] Klimesch W, Sauseng P, Gerloff C. Enhancing cognitive performance with repetitive transcranial magnetic stimulation at human individual alpha frequency. Eur J Neurosci 2003;17:1129–33. https://doi.org/10.1046/j.1460-9568.2003.02517.x.

[53] Grandy TH, Werkle-Bergner M, Chicherio C, Schmiedek F, Lövdén M, Lindenberger U. Peak individual alpha frequency qualifies as a stable neurophysiological trait marker in healthy younger and older adults. Psychophysiology 2013;50:570–82. https://doi.org/10.1111/psyp.12043.

[54] Haegens S, Cousijn H, Wallis G, Harrison PJ, Nobre AC. Inter- and intra-individual variability in alpha peak frequency. NeuroImage 2014;92:46–55. https://doi.org/10.1016/j.neuroimage.2014.01.049.

[55] Gray MJ, Emmanouil TA. Individual alpha frequency increases during a task but is unchanged by alpha-band flicker. Psychophysiology 2020;57:e13480. https://doi.org/10.1111/psyp.13480.

[56] Wutz A, Melcher D, Samaha J. Frequency modulation of neural oscillations according to visual task demands. Proc Natl Acad Sci U S A 2018;115:1346–51. https://doi.org/10.1073/pnas.1713318115.

[57] Bollimunta A, Mo J, Schroeder CE, Ding M. Neuronal mechanisms and attentional modulation of corticothalamic alpha oscillations. J Neurosci 2011;31:4935–43. https://doi.org/10.1523/JNEUROSCI.5580-10.2011.

[58] Bollimunta A, Chen Y, Schroeder CE, Ding M. Neuronal mechanisms of cortical alpha oscillations in awake-behaving macaques. J Neurosci 2008;28:9976–88. https://doi.org/10.1523/JNEUROSCI.2699-08.2008.

575 [59] Tallon-Baudry C, Bertrand O. Oscillatory gamma activity in humans and its role in object
576 representation. Trends Cogn Sci 1999;3:151–62.
577 [60] Rossi S, Hallett M, Rossini PM, Pascual-Leone A, of TMS Consensus Group TS. Safety, ethical
578 considerations, and application guidelines for the use of transcranial magnetic stimulation in clinical
579 practice and research. Clin Neurophysiol 2009;120:2008–39.
580 https://doi.org/10.1016/j.clinph.2009.08.016.
581 [61] Brainard DH. The psychophysics toolbox. Spat Vis 1997;10:433–6.
582 [62] Pelli DG. The VideoToolbox software for visual psychophysics Transforming numbers into movies.
583 Spat Vis 1997;10:437–42.
584 [63] Macmillan NA, Creelman CD. Detection theory A user's guide. 2nd ed. Mahwah: Lawrence Erlbaum
585 Associates, Inc.; 2004.
586 [64] Green DM, Swets JA. Signal detection theory and psychophysics. New York: John Wiley & Sons, Inc.;
587 1966.
588 [65] Cousineau D. Confidence intervals in within-subject designs A simpler solution to Loftus and Masson's
589 method. Tutor Quant Methods Psychol 2005;1:42–5.
590 [66] Welch PD. The use of fast Fourier transform for the estimation of power spectra A method based on
591 time averaging over short, modified periodograms. IEEE Trans Audio Electroacoustics 1967;15:70–3.
592 [67] Oostenveld R, Fries P, Maris E, Schoffelen J-M. FieldTrip Open source software for advanced analysis
593 of MEG, EEG, and invasive electrophysiological data. Comput Intell Neurosci 2011;2011:156869.
594 https://doi.org/10.1155/2011/156869.
595 [68] Tadel F, Baillet S, Mosher JC, Pantazis D, Leahy RM. Brainstorm A user-friendly application for
596 MEG/EEG analysis. Comput Intell Neurosci 2011;2011:879716. https://doi.org/10.1155/2011/879716.
597 [69] Lachaux J-P, Rodriguez E, Martinerie J, Varela FJ. Measuring phase synchrony in brain signals. Hum
598 Brain Mapp 1999;8:194–208.
599 [70] Maris E, Oostenveld R. Nonparametric statistical testing of EEG- and MEG-data. J Neurosci Methods
600 2007;164:177–90. https://doi.org/10.1016/j.jneumeth.2007.03.024.
601 [71] Paus T, Sipila PK, Strafella AP. Synchronization of neuronal activity in the human primary motor cortex
602 by transcranial magnetic stimulation An EEG study. J Neurophysiol 2001;86:1983–90.
603 https://doi.org/10.1152/jn.2001.86.4.1983.
604 [72] Rosanova M, Casali A, Bellina V, Resta F, Mariotti M, Massimini M. Natural frequencies of human
605 corticothalamic circuits. J Neurosci 2009;29:7679–85. https://doi.org/10.1523/JNEUROSCI.0445-
606 09.2009.
607 [73] Barzegaran E, Vildavski VY, Knyazeva MG. Fine structure of posterior alpha rhythm in human EEG
608 Frequency components, their cortical sources, and temporal behavior. Sci Rep 2017;7:8249.
609 https://doi.org/10.1038/s41598-017-08421-z.
610 [74] de Graaf TA, Gross J, Paterson G, Rusch T, Sack AT, Thut G. Alpha-band rhythms in visual task
611 performance Phase-locking by rhythmic sensory stimulation. PLoS ONE 2013;8:e60035.
612 https://doi.org/10.1371/journal.pone.0060035.

[75] Mathewson KE, Fabiani M, Gratton G, Beck DM, Lleras A. Rescuing stimuli from invisibility Inducing a momentary release from visual masking with pre-target entrainment. Cognition 2010;115:186–91. https://doi.org/10.1016/j.cognition.2009.11.010.

[76] Dugué L, Roberts M, Carrasco M. Attention reorients periodically. Curr Biol 2016;26:1595–601. https://doi.org/10.1016/j.cub.2016.04.046.

[77] Iemi L, Chaumon M, Crouzet SM, Busch NA. Spontaneous neural oscillations bias perception by modulating baseline excitability. J Neurosci 2017;37:807–19. https://doi.org/10.1523/JNEUROSCI.1432-16.2016.

[78] Limbach K, Corballis PM. Prestimulus alpha power influences response criterion in a detection task. Psychophysiology 2016;53:1154–64. https://doi.org/10.1111/psyp.12666.

[79] Sherman MT, Kanai R, Seth AK, VanRullen R. Rhythmic influence of top-down perceptual priors in the phase of prestimulus occipital alpha oscillations. J Cogn Neurosci 2016;28:1318–30. https://doi.org/10.1162/jocn_a_00973.

[80] Samaha J, Iemi L, Postle BR. Prestimulus alpha-band power biases visual discrimination confidence, but not accuracy. Conscious Cogn 2017;54:47–55. https://doi.org/10.1016/j.concog.2017.02.005.

[81] Zaehle T, Rach S, Herrmann CS. Transcranial alternating current stimulation enhances individual alpha activity in human EEG. PLoS ONE 2010;5:e13766. https://doi.org/10.1371/journal.pone.0013766.

[82] Helfrich RF, Schneider TR, Rach S, Trautmann-Lengsfeld SA, Engel AK, Herrmann CS. Entrainment of brain oscillations by transcranial alternating current stimulation. Curr Biol 2014;24:333–9. https://doi.org/10.1016/j.cub.2013.12.041.

[83] Haberbosch L, Schmidt S, Jooss A, Köhn A, Kozarzewski L, Rönnefarth M, et al. Rebound or entrainment? The influence of alternating current stimulation on individual alpha. Front Hum Neurosci 2019;13:43. https://doi.org/10.3389/fnhum.2019.00043.

[84] Vossen A, Gross J, Thut G. Alpha power increase after transcranial alternating current stimulation at alpha frequency (α-tACS) reflects plastic changes rather than entrainment. Brain Stimulat 2015;8:499–508. https://doi.org/10.1016/j.brs.2014.12.004.

Table 1. p values of planned t-tests of evoked oscillation amplitude and ITPC at the α-band. The frequency of interest is 10 Hz. The electrode of interest is the average of O2 and PO4 (near the stimulation loci; see **Figure 1C**). The time windows include the periods before (W0), during (W1-W3), and after (W4-W6) stimulation. The contrasts are significant starting from W2 until W5 or W6. *: p<.05, **: p<.01, ***: p<.001

Time windows	W0	W1	W2	W3	W4	W5	W6
Evoked amplitude	n.s.	n.s.	.030*	.015*	.021*	.031*	n.s.
ITPC	n.s.	n.s.	.030*	.004**	.005**	.009**	.013*

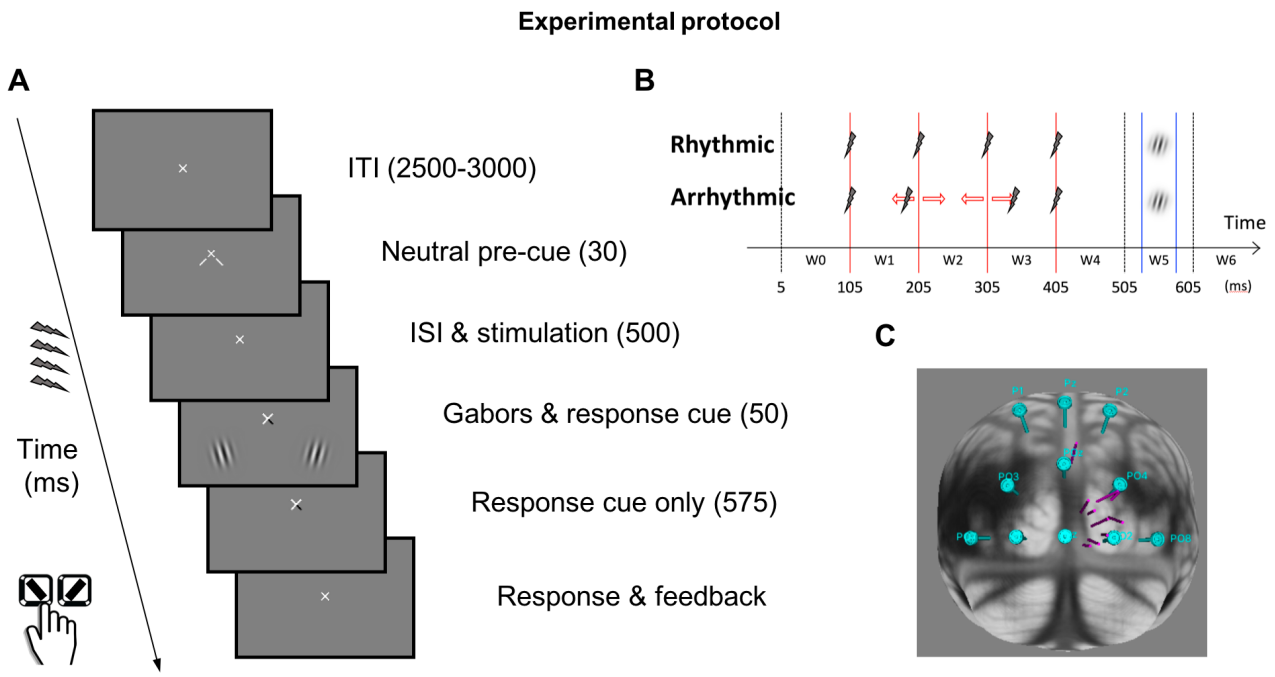

Figure 1. Experimental protocol (**A**), Trial structure. Each trial began with an intertrial period (ITI), followed by a neutral pre-cue to indicate the two stimulus locations. Active or sham stimulation was delivered in the interstimulus interval (ISI) between the neural pre-cue and the Gabor stimuli. The response cue indicated which Gabor was the target. Participants responded whether the target Gabor was tilted to the left or to the right with a key press. (**B**), Stimulation patterns & analysis time windows. The onset of the pre-cue is at t = 0. The four red lines mark the pulse timings in the rhythmic condition. The two blue lines mark the timings of Gabors onset and offset. In the rhythmic condition, the gap between pulses was exactly 100 ms. In the arrhythmic condition, the timing of the second and the third pulses was jittered (see text and Fig S1 for the probability distribution). Time window W0 is the cycle before the first pulse. Time windows W1, W2, and W3 are the cycles between pulse pairs. Time windows W4 and W5 are the first and the second cycles after the last pulse, respectively. (**C**), TMS loci & directions. Each cylinder represents the TMS directional vector of one participant on the MNI brain template. The cyan discs indicate the EEG electrode positions.

Time-frequency analysis of phase-locked activities

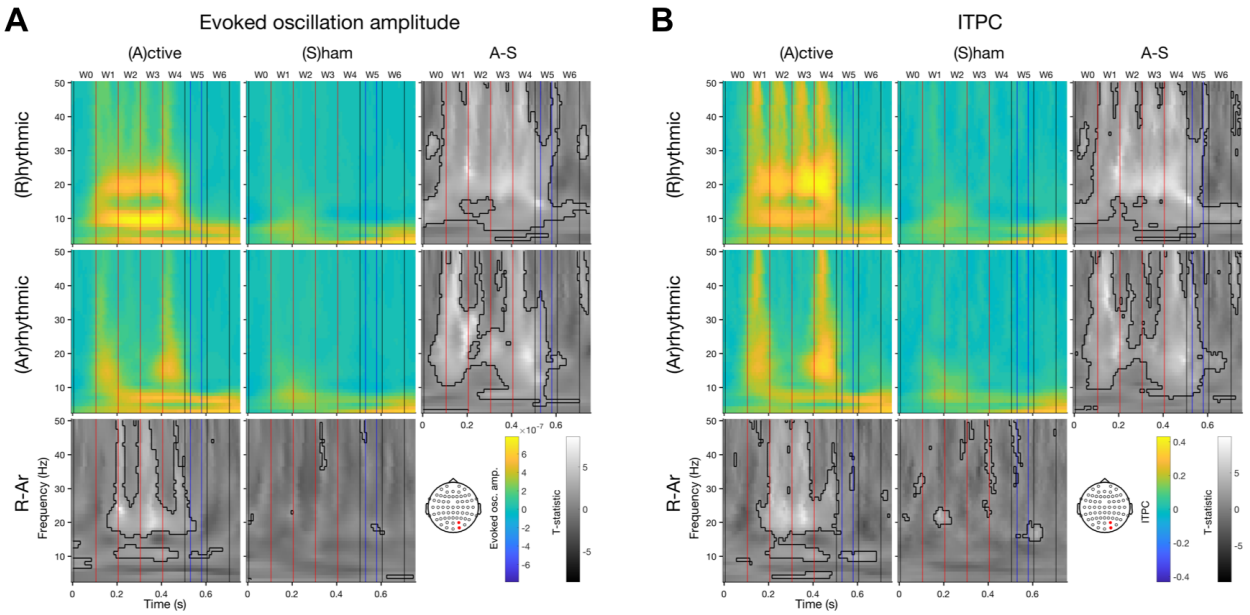

Figure 2. Time-frequency analysis of phase-locked activities. Colored panels are the group-averaged activities per condition (rhythmic vs. arrhythmic × active vs. sham stimulation). Gray panels are the t-statistics of condition contrasts per column or row. The precue onset was defined as t=0. The electrode of interest is the average the two channels (O2 & PO4) near the TMS loci. In the t-statistic panels, the thick black contours indicate significant time-frequency bins. In each panel, the vertical black and red lines demarcate the 100 ms time windows, blue lines the Gabor onset and offset. The red lines are also the pulse timings in the rhythmic conditions. (**A**), evoked oscillation amplitude. (**B**), ITPC. Each TMS pulse elicits broad band responses. Rhythmic-active stimulation elicits activities around 10 Hz and the first harmonic. Note that the arrhythmic-active condition is a more stringent control than the rhythmic-sham condition for the rhythmic-active condition. Note that at 10 Hz, the full width at half maximum of time and frequency for Morlet wavelets with c=5 are 0.19 and 4.71, respectively.

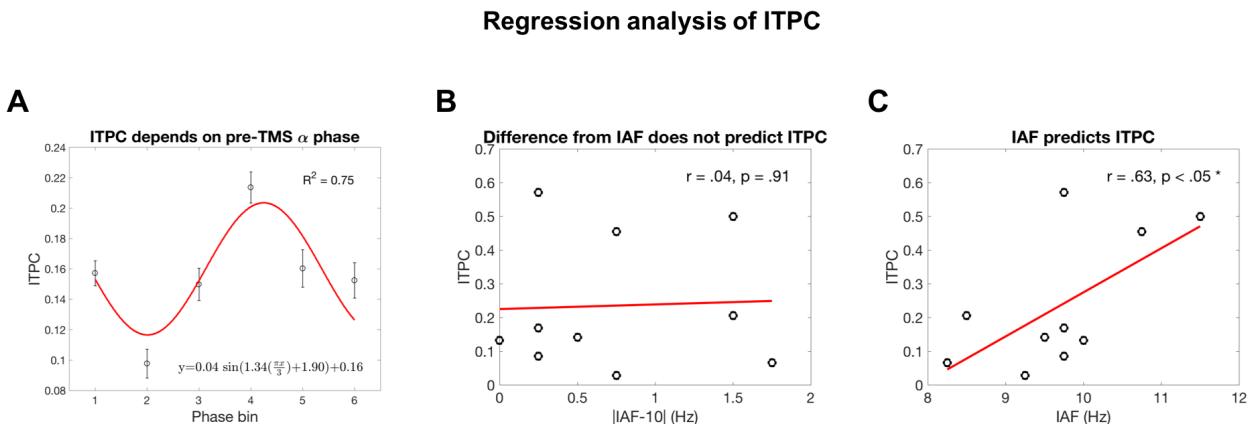

Figure 3. Regression analysis of ITPC in the rhythmic-active stimulation condition. The time window of ITPC is 0.205-0.705 s, the same as the significant windows in **Table 1**. (**A**), ITPC depends on pre-TMS α-phase (200 ms before the first pulse). Each point is the average of 510 samples (10 participants x 51 time points). The error bars represent ±1 SEM. This ~1 period cyclic pattern suggests that the congruency between TMS and the phase of ongoing α oscillations determines the effectiveness of entrainment. (**B**), Difference from IAF does not predict ITPC. The absolute difference between IAF and the entraining frequency does not predict ITPC during and after stimulation. (**C**), IAF predicts ITPC. IAF positively correlates with ITPC during and after stimulation. See text for discussion.

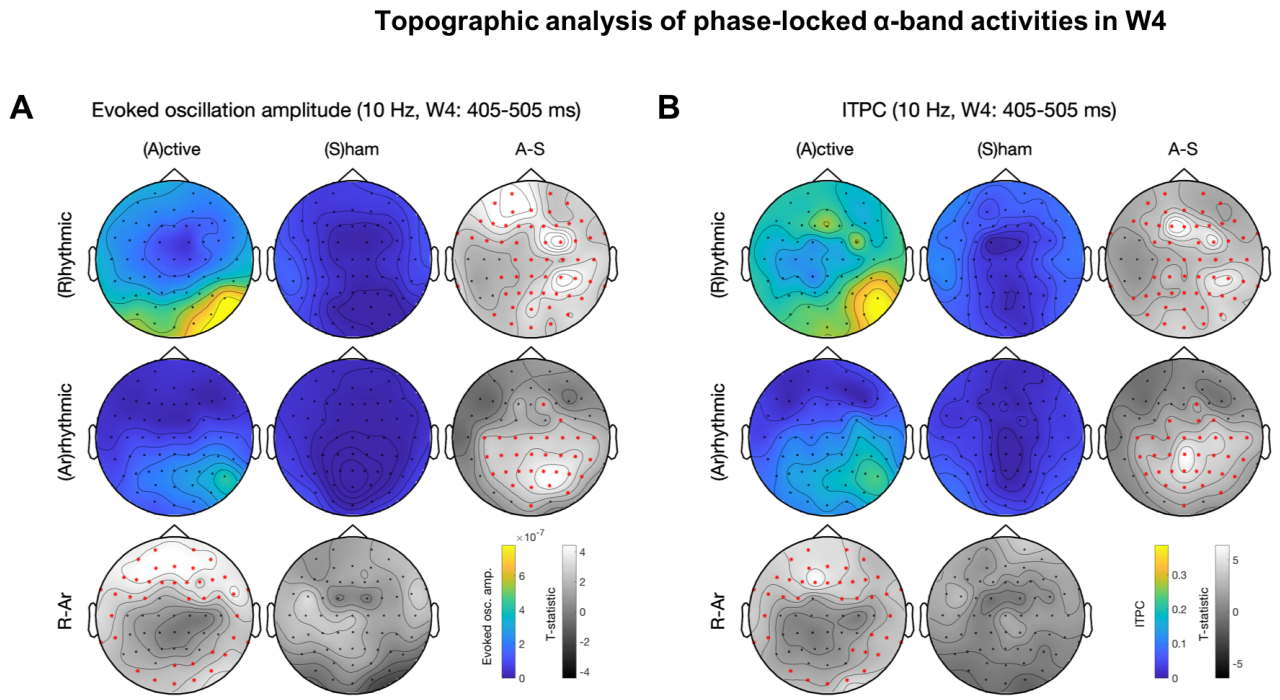

Figure 4. Topographic analysis of phase-locked α-band activities in W4. The panel layout is similar to that in **Figure 2**. The red star symbols indicate significant channels after cluster-based permutation test for multiple comparison correction. (**A**), evoked oscillation amplitude. (**B**), ITPC. Rhythmic-active stimulation elicits widespread activation. With arrhythmic-active stimulation as control, there are significant clusters in the frontal and the occipital regions. Note that the patterns between (**A**) and (**B**) are similar.

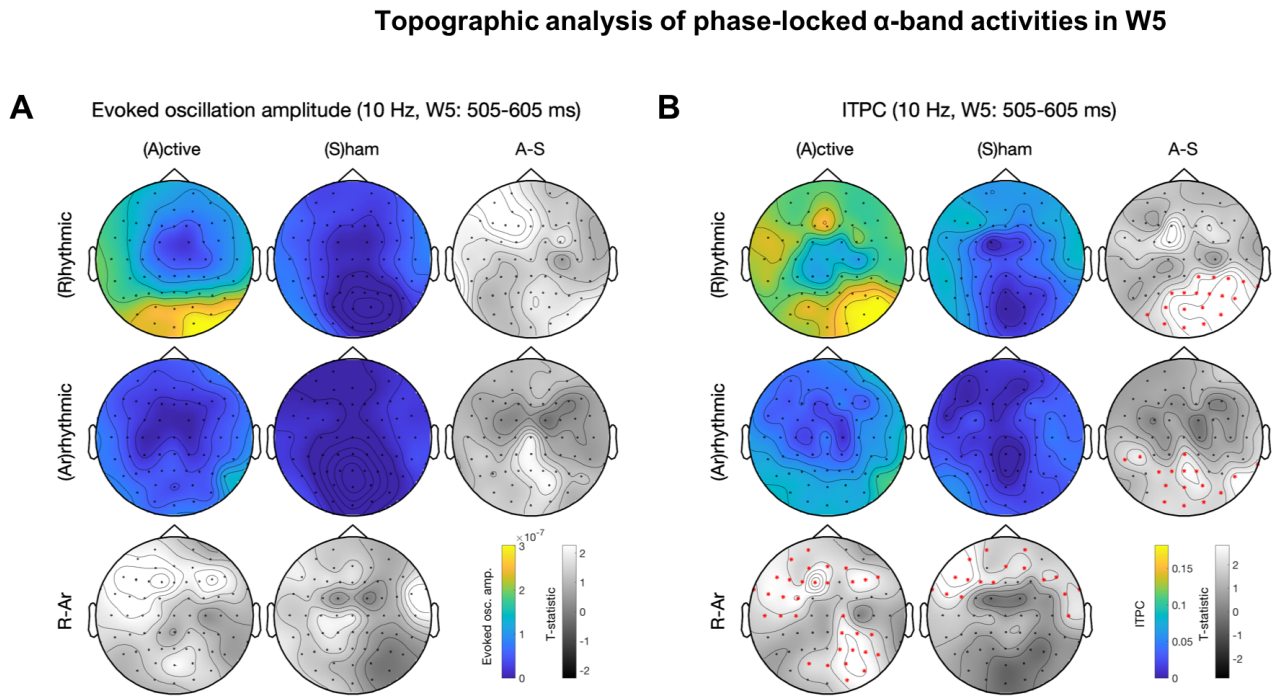

Figure 5. Topographic analysis of phase-locked α-band activities in W5. See **Figure 4** for panel layout description. (**A**), evoked oscillation amplitude. (**B**), ITPC. Rhythmic-active stimulation elicits widespread activation. Note that (**B**) continues to show significant difference between conditions whereas (**A**) does not.

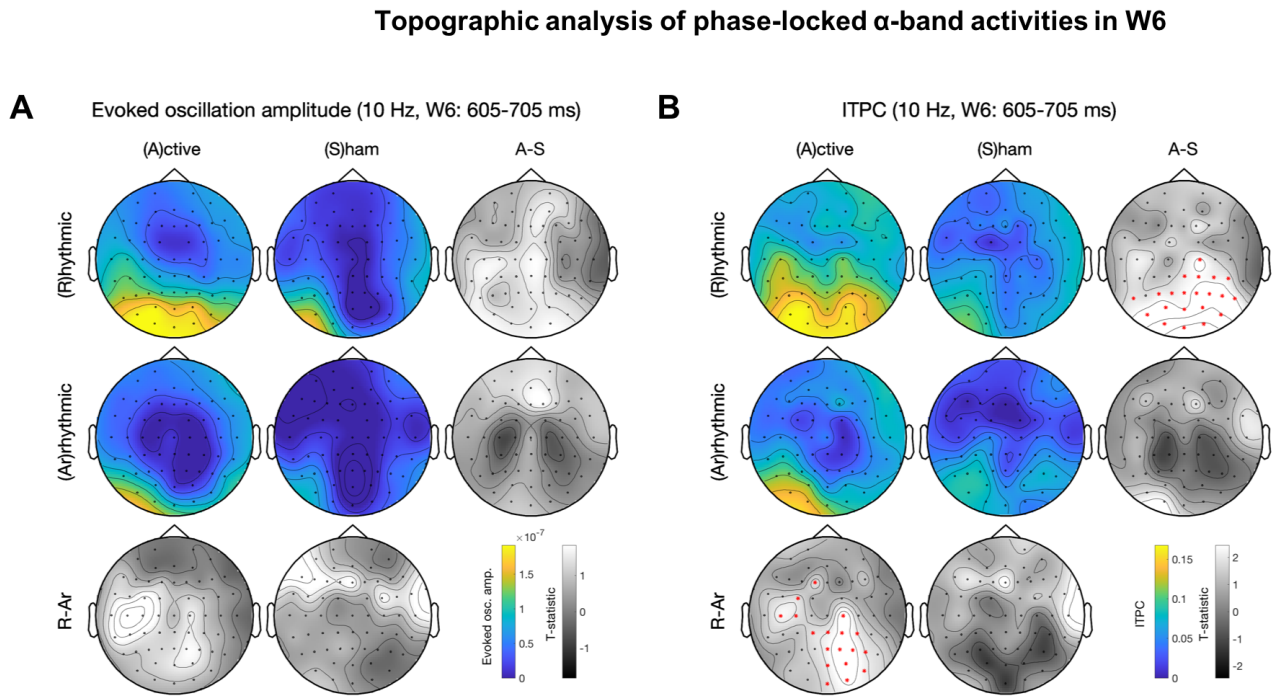

Figure 6. Topographic analysis of phase-locked α-band activities in W6. See **Figure 4** for panel layout description. (**A**), evoked oscillation amplitude. (**B**), ITPC. Rhythmic-active stimulation elicits widespread activation. Note that (**B**) continues to show significant difference between conditions whereas (**A**) does not. A significant lateralized parieto-occipital cluster exists in the rhythmic- vs. arrhythmic-active stimulation contrast.